2008

Late endocytic multivesicular bodies intersect the chlamydial inclusion in the absence of CD63

Wandy L. Beatty
Washington University School of Medicine in St. Louis

Infection and Immunity

Late Endocytic Multivesicular Bodies Intersect the Chlamydial Inclusion in the Absence of CD63

Wandy L. Beatty
Infect. Immun. **2008, 76(7):2872. DOI: 10.1128/IAI.00129-08.**
Published Ahead of Print 21 April 2008.

INFECTION AND IMMUNITY, July 2008, p. 2872–2881 Vol. 76, No. 7
0019-9567/08/$08.00+0 doi:10.1128/IAI.00129-08

Late Endocytic Multivesicular Bodies Intersect the Chlamydial Inclusion in the Absence of CD63[▽]

Wandy L. Beatty*

Department of Molecular Microbiology, Washington University School of Medicine, St. Louis, Missouri 63110

Received 30 January 2008/Returned for modification 13 March 2008/Accepted 14 April 2008

Chlamydiae are obligate intracellular bacterial pathogens that replicate solely within a membrane-bound vacuole termed an inclusion. Within the confines of the inclusion, the replicating bacteria acquire amino acids, nucleotides, and other precursors from the host cell. Trafficking from CD63-positive multivesicular bodies to the inclusion was previously identified as a novel interaction that provided essential precursors for the maintenance of a productive intracellular infection. The present study analyzes the direct delivery of resident protein and lipid constituents of multivesicular bodies to the intracellular chlamydiae. The manipulation of this trafficking pathway with an inhibitor of multivesicular body transport and the delivery of exogenous antibodies altered protein and cholesterol acquisition and delayed the maturation of the chlamydial inclusion. Although inhibitor studies and ultrastructural analyses confirmed a novel interaction between CD63-positive multivesicular bodies and the intracellular chlamydiae, neutralization with small interfering RNAs and anti-CD63 Fab fragments revealed that CD63 itself was not required for this association. These studies confirm CD63 as a constituent in multivesicular body-to-inclusion transport; however, other requisite components of these host cell compartments must control the delivery of key nutrients that are essential to intracellular bacterial development.

Chlamydiae are obligate intracellular bacteria recognized for their etiologic association with a broad spectrum of clinically distinct manifestations, extending from acute self-limiting ocular and genital infections to chronic inflammatory diseases that lead to blindness or infertility. The success of chlamydiae hinges upon the complex host-pathogen interaction that is mediated by the invading bacteria. Upon internalization into the host cell, chlamydiae replicate within a membrane-bound inclusion. Within this environment, these bacterial pathogens orchestrate the expansion of the inclusion and the generation/acquisition of biosynthetic constituents that are essential for their propagation and subsistence.

Beyond the confines of the inclusion membrane is the nutrient-rich host cell cytoplasm. Although chlamydiae remain largely dissociated from the host cytosol, the recruitment of key regulators of membrane trafficking (20, 22) and the association with nutrient-rich eukaryotic organelles suggest an interaction that is not passive. Among these interactions is the intersection of the inclusion with a subset of vesicles originating from the *trans*-Golgi network. Golgi-derived sphingomyelin and cholesterol destined for the plasma membrane are diverted to the chlamydial inclusion and are incorporated into bacterial cell walls (6, 9, 10, 23). In addition, chlamydiae target lipid droplets, neutral lipid-rich eukaryotic organelles that may serve as conduits for the transport of essential lipids or vesicular transport proteins to the chlamydial inclusion (18).

The present study focuses on the host cell's multivesicular bodies (MVBs) as a source of essential constituents for the intracellular propagation of *Chlamydia trachomatis*. MVBs are lipid- and cholesterol-rich late endocytic organelles that are pivotal in the segregation of host-derived lipids and proteins (7, 21). CD63-positive MVBs previously have been shown to intersect the chlamydial inclusion and provide lipids that are essential for the maintenance of a productive intracellular infection (3). Utilizing ultrastructural analyses and extending inhibitor studies to incorporate small interfering RNA (siRNA) and exogenous Fab fragments, the intersection between MVBs and intracellular *Chlamydia* was confirmed to proceed independently of CD63.

MATERIALS AND METHODS

Reagents. H5C6, a mouse monoclonal antibody against human CD63, and H4A3, a mouse monoclonal antibody against human LAMP-1, were developed by J. Thomas August and James E. K. Hildreth (John Hopkins University School of Medicine, Baltimore, MD) and obtained from the Developmental Studies Hybridoma Bank/NICHD (University of Iowa, Iowa City). 6C4, a mouse monoclonal antibody generated to lysobisphosphatidic acid (LBPA), was generously provided by Toshihide Kobayashi and Jean Gruenberg (University of Geneva, Geneva, Switzerland). A57B9, a mouse monoclonal antibody against the chlamydial heat shock protein 60 (hsp60), was kindly provided by Richard Morrison (University of Arkansas, Little Rock). TOPRO-3, Lysotracker Red, and kits for Alexa Fluor protein labeling and biotin protein labeling were obtained from Invitrogen (Carlsbad, CA). Filipin and 3-β-(2-diethylaminoethoxy)-androstenone HCl (U18666A) were obtained from Sigma (St. Louis, MO). Nontargeting and human CD63-specific siRNAs and DharmaFECT1 were purchased from Dharmacon, Inc. (Lafayette, CO). Streptavidin gold conjugates were obtained from Ted Pella Inc. (Redding, CA). Fluorescein-conjugated goat anti-mouse immunoglobulin G (IgG) Fab fragment-specific antibody and colloidal gold-conjugated anti-mouse IgG (heavy plus light chain) antibodies were purchased from Jackson ImmunoResearch Laboratories, Inc. (West Grove, PA).

Chlamydia and cell culture. *C. trachomatis* serovar E was obtained from Harlan Caldwell (Rocky Mountain Laboratories, National Institute of Allergy and Infectious Diseases, NIH) and propagated in HEp-2 cells (ATCC, Manassas, VA). Elementary bodies (EBs) were purified by Renografin gradient centrifugation as previously described (4). HEp-2 cells were maintained at 37°C with 5.5% CO_2 in Iscove's modified Dulbecco's medium supplemented with 12.5 mM HEPES, 10% (vol/vol) fetal bovine serum (FBS), and 10 μg/ml gentamicin. HEp-2 cells were infected by incubating monolayers with *Chlamydia* EBs at a

* Mailing address: Department of Molecular Microbiology, Washington University School of Medicine, 660 South Euclid Avenue, Campus Box 8230, St. Louis, MO 63110-1093. Phone: (314) 362-4987. Fax: (314) 362-1232. E-mail: beatty@borcim.wustl.edu.
▽ Published ahead of print on 21 April 2008.

multiplicity of infection of 0.5 for 1 h at 37°C on a platform rocker. Cells were washed twice with phosphate-buffered saline (PBS) and incubated in Iscove's medium for the times indicated.

Immunofluorescence and confocal microscopy. HEp-2 cells were grown on glass coverslips or on chamber slides and infected with *Chlamydia* as described above. For immunofluorescence analysis, antibodies to CD63 and LBPA were directly conjugated with Alexa Fluor 488 and Alexa Fluor 568, respectively, using protein-labeling kits obtained from Invitrogen. Infected cells were fixed for 20 min at room temperature in 1% formaldehyde and subsequently treated for 1 min with 1 mg/ml Zwittergent. Fixed and permeable cells then were blocked in 5% goat serum–PBS and incubated with the fluorophore-conjugated primary antibodies for 20 min. Labeling with individual primary antibodies revealed the same labeling pattern as that observed with double labeling. Incubation with 0.2 μM TOPRO-3 (a monomeric cyanine nucleic acid stain, with an absorbance wavelength of 642 nm and an emission wavelength of 661 nm) for 10 min at room temperature labeled both the intracellular bacteria and host cell nuclei. Coverslips and slides were mounted using ProLong Anti-Fade mounting medium (Invitrogen). Images were acquired using a Zeiss LSM510 Meta laser-scanning confocal microscope (Carl Zeiss Inc., Thornwood, NY) equipped with a ×63, 1.4-numerical-aperture Zeiss Plan Apochromat oil objective. Orthogonal Z slices of 0.5 or 0.8 μm through the depth of the inclusion were analyzed, and slices at the center of the inclusion Z height were acquired. Corresponding intensity distribution profiles were obtained using the Zeiss LSM510 software.

For the analysis of cholesterol distribution, infected HEp-2 cells were immunolabeled as described above. Following TOPRO-3 labeling, the monolayers were washed in PBS and incubated with 50 μg/ml filipin for 20 min. Coverslips were mounted as described above and visualized with a Zeiss Axioskop Mot Plus fluorescence microscope equipped with a ×100, 1.4-numerical-aperture Zeiss Plan Apochromat oil objective. Images were acquired using Axiovision software (Carl Zeiss Inc).

Electron microscopy. For the analysis of CD63 and LBPA localization at the ultrastructural level, *Chlamydia*-infected cells were prepared for cryoimmunoelectron microscopy. Infected cells were fixed in 4% paraformaldehyde–0.1% glutaraldehyde (Polysciences Inc., Warrington, PA) in 100 mM piperazine-*N*,*N*′-bis(2-ethanesulfonic acid) (PIPES)–0.5 mM $MgCl_2$, pH 7.2, for 1 h at 4°C. Samples then were embedded in 10% gelatin and infiltrated overnight with 2.3 M sucrose–20% polyvinyl pyrrolidone in PIPES-$MgCl_2$ at 4°C. Samples were trimmed, frozen in liquid nitrogen, and sectioned with a Leica Ultracut UCT cryoultramicrotome (Leica Microsystems Inc., Bannockburn, IL).

For single labeling with anti-CD63 antibody, 50-nm sections were blocked with 5% FBS–5% goat serum for 30 min and then were incubated with the primary antibody. Sections then were washed in block buffer and probed with anti-mouse 18-nm colloidal gold-conjugated secondary antibody (Jackson ImmunoResearch Laboratories). For double-labeling experiments, sections were sequentially labeled with anti-LBPA followed by anti-mouse 12-nm colloidal gold-conjugated secondary antibody. Sections then were labeled with biotinylated anti-CD63 antibody followed by streptavidin-conjugated 20-nm colloidal gold. Immunolabeled sections were washed in PIPES buffer, followed by an extensive water rinse, and were stained with 1% uranyl acetate–1.6% methyl cellulose (Ted Pella Inc.). Samples were viewed with a JEOL 1200EX transmission electron microscope (JEOL USA Inc., Peabody, MA). All labeling experiments were conducted in parallel, with controls omitting the primary antibody. These controls were consistently negative at the concentration of colloidal gold-conjugated secondary antibody or streptavidin used in these studies.

Analysis of inhibitors. To analyze the inhibitors, HEp-2 cells were infected with *Chlamydia* as described above. One hour postinfection, cells were washed with PBS and incubated with Iscove's medium containing 10 μM U18666A, an inhibitor of MVB transport (19), for the 48-h time course of infection. The effects of inhibitors on inclusion development and morphology were determined by infectivity assays and immunofluorescence analysis. The effects on cholesterol trafficking were determined by the analysis of filipin distribution.

RNA interference. HEp-2 cells at subconfluency were transfected with control (siCONTROL Non-Targeting siRNA no. 1; designated siControl) or CD63-specific (ON-TARGETplus SMARTpool, human CD63; designated siCD63) siRNA, using DharmaFECT1 as the transfection agent as described in the manufacturer's protocol (Dharmacon, Inc.). Cells transfected for 24 h then were infected with *Chlamydia* as described above. One hour postinfection, cells were subjected to a second transfection and were analyzed at 48 h postinfection by fluorescence and electron microscopy.

Infectivity assays. At 48 h postinfection, infected monolayers cultured in the presence of inhibitors were washed with PBS, scraped from the culture dishes into fresh Iscove's medium, and sonicated to disrupt the HEp-2 cells and release infectious EBs. Dilutions of the disrupted cell suspensions were inoculated onto fresh monolayers of HEp-2 cells as described above. At 48 h postinfection, the monolayers were fixed, immunolabeled with anti-chlamydial hsp60 antibody, and visualized with a Zeiss Axioskop Mot Plus fluorescence microscope to quantitate the number of infection-forming units. Data are presented as the mean infection-forming units of triplicate cultures ± standard deviations (SD). *P* values were determined using a *t* test with a 95% confidence interval.

Exogenous antibody loading. Anti-CD63 Fab fragments were generated and purified using a mouse IgG1 Fab preparation kit (Pierce Biotechnology, Rockford, IL). Briefly, 1 mg/ml of mouse anti-CD63 IgG1 was dissolved in the provided digestion buffer, which was supplemented with 10 mM cysteine. The IgG sample was equilibrated with immobilized ficin protease and purified according to the manufacturer's instructions. Protein A columns were used to bind Fc fragments and undigested IgG, allowing for the separation of Fab fragments. Nonreducing sodium dodecyl sulfate–10% polyacrylamide gel electrophoresis (SDS–10% PAGE) was used to confirm complete digestion to monovalent Fab fragments and the purity of the preparation.

To minimize the volume of exogenous antibody utilized in these studies, HEp-2 cells were grown in chamber slides. Untransfected cells, or cells transfected with siControl or siCD63 RNA as described above, were infected with *C. trachomatis*. Twenty-four hours postinfection, cells were washed with PBS and incubated in Iscove's medium containing 40 μg/ml anti-LAMP1 antibody, anti-CD63 antibody, or purified anti-CD63 Fab fragments. At 48 h postinfection, where indicated, cells were incubated with 1 μM Lysotracker Red for 10 min at 37°C to identify lysosomal compartments. Cells then were fixed and immunolabeled with Alexa Fluor 488-conjugated mouse antibody or fluorescein-conjugated goat anti-mouse IgG Fab fragment-specific antibody to detect the uptake of exogenous antibodies. For the analysis of cholesterol distribution, cells were incubated with 50 μg/ml filipin for 20 min. Cells then were labeled with TOPRO-3 and mounted as described above. Orthogonal Z slices of 0.5 or 0.8 μm (wider slices were used because of the lower labeling intensity with fluorescein-conjugated Fab-specific secondary antibody) through the depth of the inclusion were analyzed, and slices at the center of the inclusion Z height were acquired. For the quantitative comparison of the effects of exogenous antibodies on inclusion size, random fields were selected and confocal images of 0.8 μm thickness were obtained. The LSM510 software was used to trace and determine the cross-sectional area (in square micrometers) of 50 inclusions for each condition.

RESULTS

CD63 and LBPA localize to the chlamydial inclusion in infected HEp-2 cells. To evaluate the intersection between the chlamydial inclusion and late endocytic MVBs, the distributions of two MVB constituents, CD63 and LBPA, were analyzed in *C. trachomatis*-infected cells. CD63 and LBPA both showed specific localization at the site of the chlamydial inclusion by confocal microscopy analysis (Fig. 1), as described previously (3). This association was demonstrated in HEp-2 cells infected with *C. trachomatis* serovar E and labeled by direct immunofluorescence using antibodies specific to these markers. The confocal analysis of midplane Z sections through the center of the inclusion revealed a fine punctate pattern at the site of the chlamydial inclusion (Fig. 1), which colocalized with TOPRO-3-labeled bacteria within the inclusion. In addition, TOPRO-3-labeled host cell nuclei did not specifically label with antibodies to MVBs, providing an internal control for the level of background label. The distribution of these markers was shown quantitatively by generating a profile of the intensity distribution of each constituent along a line traversing the chlamydial inclusion (Fig. 1). Anti-CD63 and anti-LBPA antibodies clearly colocalized with TOPRO-3-labeled chlamydiae within the profile of the inclusion while being excluded from the TOPRO-3-labeled host cell nuclei.

The association of CD63 and LBPA with the chlamydial inclusion is not clearly apparent by confocal microscopy until 36 to 48 h postinfection (3). This indicates that these constituents must accumulate within the inclusion, throughout the

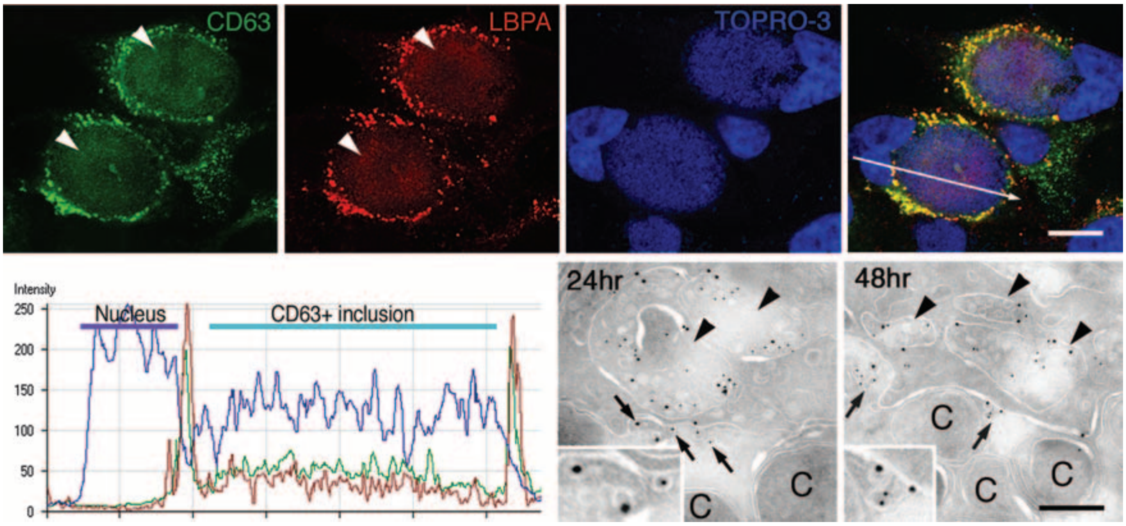

FIG. 1. CD63 and LBPA localize to the chlamydial inclusion by immunofluorescence and immunoelectron microscopy. HEp-2 cells were infected with *C. trachomatis* E for 24 and 48 h, immunolabeled with the indicated MVB-specific antibodies, and analyzed by confocal and electron microscopy. (Upper) Optical sections (0.5 μm thick) of infected cells immunolabeled with anti-CD63-Alexa Fluor 488 and anti-LBPA-Alexa Fluor 568. The TOPRO-3 labeling of the equivalent confocal slice identified intracellular bacteria and host cell nuclei (merged image). Arrowheads identify chlamydial inclusions. The white line in the merged image indicates the position of the profile line used for the analysis of intensity distribution. Scale bar, 20 μm. (Lower) The graph on the left shows that the intensity distribution profiles confirmed that CD63 (green line) and LBPA (red line) had high intensity values peripheral to the inclusion and also displayed intensity levels above background at the site of the TOPRO-3-positive (blue line) chlamydial inclusion. The profile through the host cell nuclei indicates the background intensity levels of CD63 and LBPA. The images on the right show cells that were infected for 24 and 48 h and immunolabeled with anti-LBPA (12 nm colloidal gold) and anti-CD63 (20-nm colloidal gold) antibodies, revealing the presence of these two constituents adjacent to the chlamydial inclusion within compartments that morphologically resembled MVBs (arrowheads). CD63 and LBPA also were evident along the inclusion membrane and in small vesicles within the inclusion lumen (arrows and enlarged in insert). C, *Chlamydia*. Scale bar, 0.5 μm.

time course of infection, to levels detectable by this technique. To confirm the presence of CD63 and LBPA within the chlamydial inclusion and to better define this interaction temporally, infected cells were analyzed at the ultrastructural level using immunoelectron microscopy. Labeling cryosections of cells that were infected with *Chlamydia* for 24 and 48 h with anti-CD63 and anti-LBPA antibodies revealed the presence of these constituents within multivesicular organelles adjacent to the chlamydial inclusion (Fig. 1, lower). In addition, immunolabeling clearly showed CD63 and LBPA within the chlamydial inclusion at both 24 and 48 h postinfection. This association at the earlier time point of 24 h postinfection indicated that transport is not a force-driven process that results from the compression of MVBs at the cell periphery by the expanding inclusion.

An inhibitor of MVB biogenesis disrupts CD63 transport and inclusion maturation. The pharmacological agent U18666A inhibits lipid transport from late endocytic compartments (19) and disrupts the trafficking of MVB-associated membrane proteins (11, 14, 16). A previous analysis of the effect of U18666A on *Chlamydia*-infected cells by fluorescence microscopy revealed the inhibition of CD63 acquisition by the chlamydial inclusion (3). In this study, the association of CD63 with the chlamydial inclusion was extended to the ultrastructural level using immunoelectron microscopy. The labeling of cryosections of cells infected with *Chlamydia* for 48 h with anti-CD63 antibodies revealed the presence of CD63 within multivesicular organelles adjacent to the chlamydial inclusion in both control and U18666A-treated cells (Fig. 2). These CD63-positive compartments appeared enlarged in cross-sections of cells treated with the inhibitor. Immunolabeling clearly showed CD63 within the chlamydial inclusions of control untreated cells (Fig. 2) but not within the inclusions of U18666A-treated cells. The U18666A inhibition of CD63 acquisition by chlamydial inclusions correlated with a disruption in the maturation of the chlamydial inclusion, characterized by a marked reduction in inclusion size and a decreased yield of infectious progeny ($P < 0.01$) (Fig. 2, right).

An inhibitor of MVB biogenesis disrupts chlamydial growth and cholesterol acquisition. MVBs are pivotal in the intracellular transport of sphingolipids and cholesterol (21), two host cell constituents that have been shown to incorporate into the chlamydial inclusion (5, 6, 10). In the present study, filipin, a fluorescent polyene antibiotic that binds the 3′ hydroxyl group of steroids, was used to analyze cholesterol distribution in *Chlamydia*-infected cells. The photoinstability of this probe prevents the quantitative detection of cholesterol incorporation, so analysis relies on comparisons between the different treatment conditions. Cholesterol was shown to accumulate at the inclusion membrane at 18 and 48 h postinfection (Fig. 3). The pharmacological agent U18666A inhibits cholesterol transport from late endocytic compartments (19). Culturing *Chlamydia*-infected cells in the presence of 10 μM U18666A for 48 h resulted in the abundant accumulation of cholesterol in swollen CD63-positive perinuclear compartments (Fig. 3, lower). Inclusion development was disrupted, as evidenced by smaller chlamydial inclusions that failed to incorporate detectable cholesterol into the inclusion membrane (Fig. 3, lower and insert). Cholesterol incorporation into inclusions of equivalent sizes (untreated and 18 h postinfection) (Fig. 3, upper) indicated that this acquisition normally occurs early in develop-

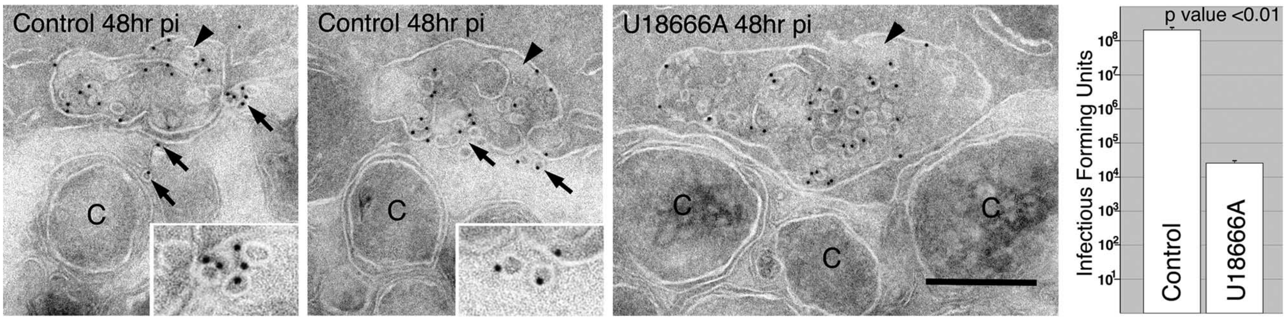

FIG. 2. Inhibitor of MVBs prevents CD63 transport to the chlamydial inclusion. HEp-2 cells were infected with *C. trachomatis* serovar E, cultured in the presence of 10 μM U18666A for 48 h, and compared to untreated cells that had been infected for 48 h. Infected cells were immunolabeled with anti-CD63 antibody (18-nm colloidal gold) and analyzed by electron microscopy. CD63 was present within compartments that morphologically resembled MVBs (arrowheads), which appeared enlarged in U18666A-treated cells. CD63 also was evident along the inclusion membrane and in small vesicles within the inclusion lumen (arrows and enlarged in inserts) in untreated control cells. CD63 was not identified within the inclusion of U18666A-treated cells. C, *Chlamydia*. Scale bar, 0.5 μm. The graph on the right shows the reduction in the recovery of infectious *Chlamydia* observed in cells cultured in the presence of U18666A, as assessed at 48 h postinfection. Data are presented as the mean infection-forming units of triplicate cultures ± SD.

ment but is blocked by U18666A treatment. The disruption of cholesterol transport to the chlamydial inclusion by the inhibition of trafficking from MVBs suggests that CD63-positive MVBs provide a novel transport pathway of cholesterol delivery to intracellular chlamydiae.

MVBs intersect the chlamydial inclusion in the absence of CD63. To determine if the MVB constituent CD63 is essential for the interaction of this compartment with the chlamydial inclusion, RNA interference studies were carried out to block CD63 synthesis. CD63 and LBPA both showed specific local-

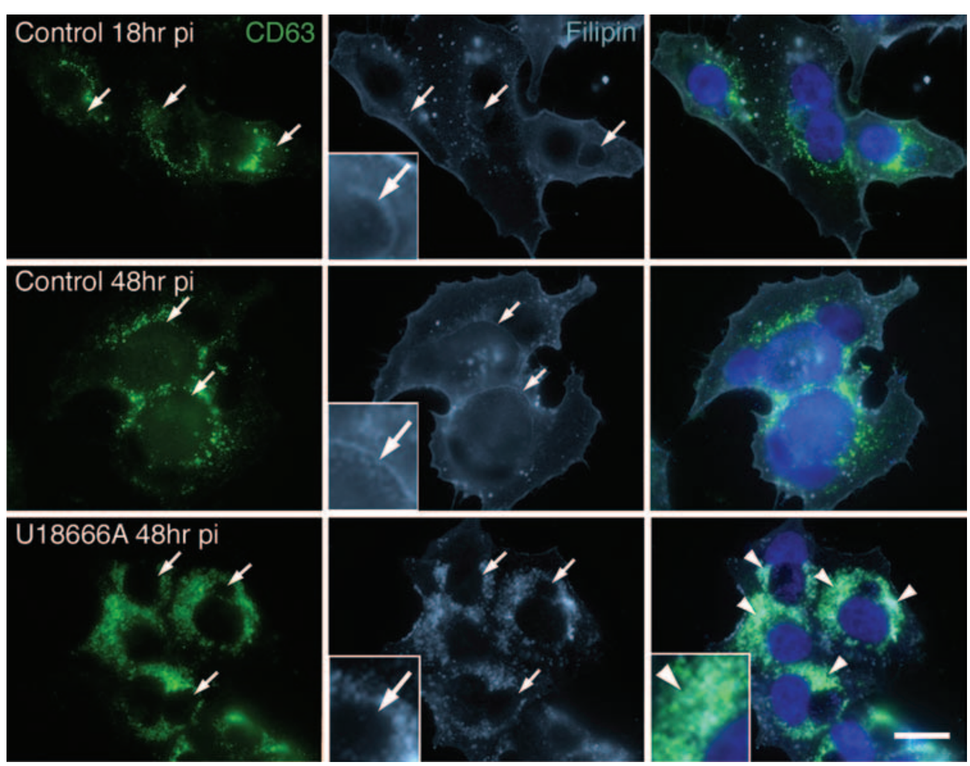

FIG. 3. Inhibitor of MVBs alters the distribution of cholesterol in *Chlamydia*-infected cells. HEp-2 cells were infected with *C. trachomatis* serovar E, cultured in the presence of 10 μM U18666A for 48 h, and compared to untreated infected cells. Infected cells were immunolabeled with anti-CD63 antibody (Alexa Fluor 488) and filipin and analyzed by fluorescence microscopy. TOPRO-3 labeling identified intracellular bacteria and host cell nuclei (merged image). (Upper) Untreated control cells at 18 h postinfection revealed the incorporation of cholesterol into the membrane of inclusions (arrows and insert) equivalent in size to those of the inclusions of cells after 48 h of inhibitor treatment. (Middle) Untreated control cells at 48 h postinfection showed the incorporation of cholesterol into the inclusion membrane (arrows and insert). (Lower) Treatment with U18666A results in the disruption of chlamydial development and the abundant accumulation of cholesterol in CD63-positive compartments (arrowheads and insert, lower right) with the lack of the incorporation of cholesterol into the chlamydial inclusion (arrows and insert, center). Scale bar, 20 μm.

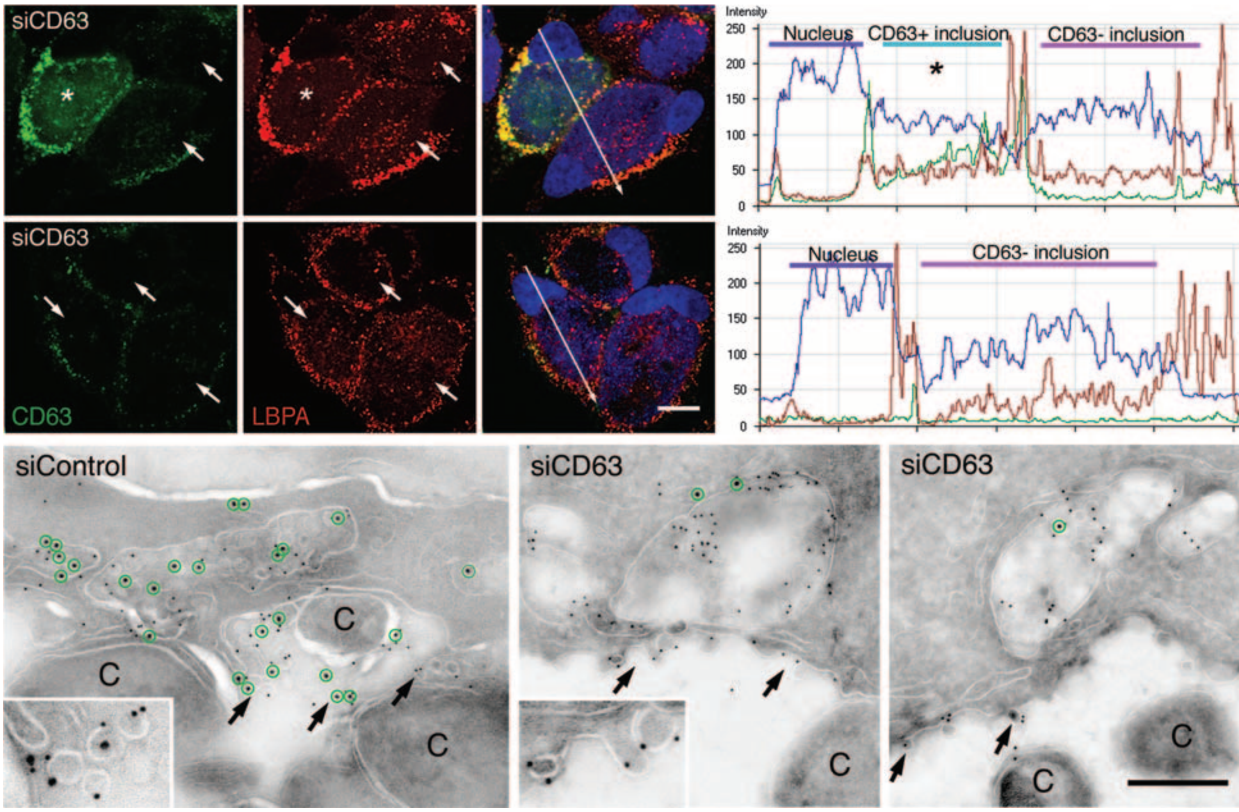

FIG. 4. siCD63 prevents the acquisition of CD63 by the chlamydial inclusion. At 48 h postinfection, HEp-2 cells transfected with siControl and siCD63 RNAs were immunolabeled with the indicated MVB-specific antibodies and analyzed by confocal and electron microscopy. (Upper) The images on the left show 0.5-μm-thick optical sections of infected cells immunolabeled with anti-CD63-Alexa Fluor 488 and anti-LBPA-Alexa Fluor 568. The TOPRO-3 labeling of the equivalent confocal slice identified intracellular bacteria and host cell nuclei (merged image). Arrows indicate transfected cells with decreased levels of CD63. The asterisk indicates an internal untransfected CD63-positive control cell. The white line in the merged image indicates the position of the profile line used for the analysis of intensity distribution. Scale bar, 20 μm. The graphs on the right show that intensity distribution profiles confirmed that CD63 (green line) and LBPA (red line) had intensity levels above background in a CD63-positive cell. In cells in which CD63 expression was reduced (arrows in the images on the left), profiles revealed a reduction of CD63 within the inclusions to background levels with no effect on the levels of LBPA. (Lower) Infected cells immunolabeled with anti-LBPA (12-nm colloidal gold) and anti-CD63 (20-nm colloidal gold) antibodies revealed the presence of CD63 (circled in green) and LBPA within the inclusion lumen (arrows and enlarged in insert) in cells transfected with the siControl RNA. In cells transfected with siCD63 RNA, the level of CD63 present in MVBs was reduced with only LBPA within the inclusion lumen. C, *Chlamydia*. Scale bar, 0.5 μm.

ization at the site of the chlamydial inclusion by confocal microscopy analysis of cells transfected with control siRNA (siControl). For cells transfected with CD63-specific siRNA (siCD63) and analyzed at 48 h postinfection, a decrease in host cell CD63 correlated with a decrease in inclusion-associated CD63 (Fig. 4, upper). The association of LBPA with perinuclear compartments and the chlamydial inclusion were not altered by siCD63. The distribution of these markers was shown quantitatively by generating a profile of the intensity distribution of each constituent along a line traversing the chlamydial inclusion (Fig. 4, upper).

The intersection of multivesicular compartments with the chlamydial inclusion was confirmed at the ultrastructural level by immunoelectron microscopy. The labeling of the cryosections of cells infected with *Chlamydia* for 48 h with anti-CD63 and anti-LBPA antibodies revealed the presence of these constituents within multivesicular organelles adjacent to the chlamydial inclusion and within the inclusion lumen in siControl cells (Fig. 4, lower). Cells transfected with siCD63 had minimal levels of CD63 within multivesicular organelles, with the protein no longer evident within the chlamydial inclusion (Fig. 4). However, LBPA was clearly present within the chlamydial inclusion of siCD63-transfected cells (Fig. 4). Although CD63-positive compartments intersect the chlamydial inclusion, RNA interference studies confirmed that CD63 itself was not required for this interaction.

Chlamydial growth and cholesterol acquisition are not altered in the absence of CD63. To determine if the MVB constituent CD63 is essential for chlamydial inclusion maturation and cholesterol acquisition, inclusion development and filipin labeling were analyzed in cells transfected with siCD63. Inclusions appeared to mature normally regardless of CD63 expression levels (Fig. 5). Cholesterol was incorporated into the inclusion membrane of cells deficient in CD63 protein (Fig. 5, insert). The recovery of infectious progeny at 48 h postinfection from siCD63-transfected cells appeared to be slightly reduced compared to that of control cells; however, this difference was not statistically significant ($P = 0.244$) (Fig. 5, right). Therefore, the intersection of MVBs and intracellular chlamydiae and the subsequent acquisition of host cell-derived

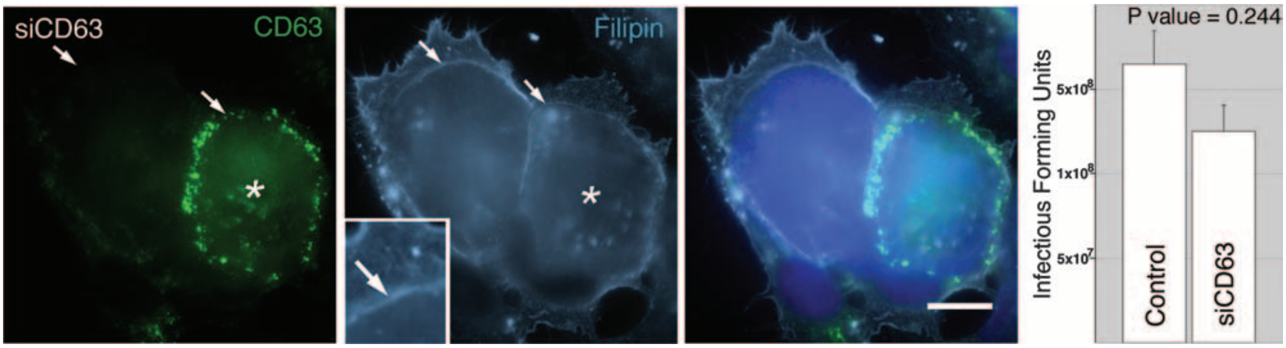

FIG. 5. siCD63 does not alter the distribution of cholesterol in *Chlamydia*-infected cells. At 48 h postinfection, HEp-2 cells transfected with siCD63 RNA were immunolabeled with the indicated anti-CD63 antibody (Alexa Fluor 488) and filipin and analyzed by fluorescence microscopy. TOPRO-3 labeling identified intracellular bacteria and host cell nuclei (merged image). No difference in the incorporation of cholesterol was evident in cells in which CD63 expression was reduced (insert) compared to that of control cells within the same field. Arrows indicate chlamydial inclusions. An asterisk indicates an internal untransfected CD63-positive control cell. Scale bar, 20 μm. The graph on the right shows that there was no significant effect of siCD63 RNA on the recovery of infectious *Chlamydia*, as assessed at 48 h postinfection. Data are presented as the mean infection-forming units of triplicate cultures ± SD.

constituents proceeds in the absence of the MVB-associated protein CD63.

Internalized exogenous anti-CD63 antibody and Fab fragments traffic to the chlamydial inclusion with disparate effects on chlamydial development. Previous studies on the neutralization of CD63 using internalized exogenous anti-CD63-specific antibody revealed an accumulation of the antibody in the chlamydial inclusion with the concurrent disruption of inclusion development (3). Those studies implied a role for CD63 in a novel MVB-inclusion interaction and are in contention with the present siRNA studies, which indicate that CD63 is not required for this association. To address this discrepancy, it was essential to confirm that the intracellular accumulation of endocytosed anti-CD63 antibody, and its subsequent association with and alteration of the chlamydial inclusion, was a consequence of direct binding to and trafficking with its antigen. siRNA studies utilizing cells transfected with siControl or siCD63 RNA were integrated with the analysis of exogenously internalized anti-CD63. In siControl cells, confocal microscopy at 48 h postinfection revealed that exogenously internalized

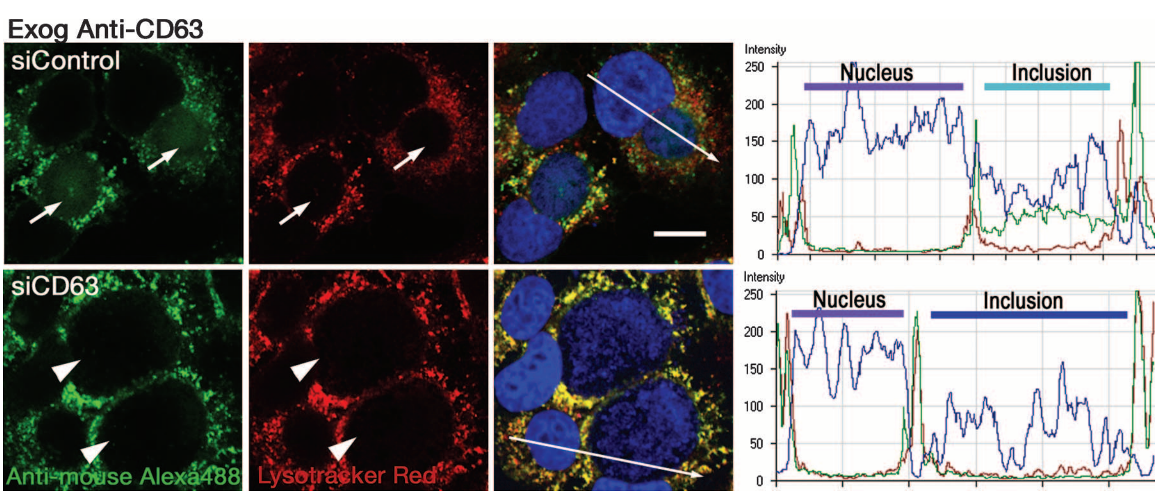

FIG. 6. siCD63 prevents the acquisition of internalized exogenous anti-CD63 antibody by the chlamydial inclusion. HEp-2 cells transfected with siControl and siCD63 RNAs were infected with *C. trachomatis* serovar E and cultured in the presence of exogenous (Exog) anti-CD63 from 24 to 48 h postinfection. (Left) Infected cells labeled with Lysotracker Red and then fixed and immunolabeled with anti-mouse Alexa Fluor 488. The TOPRO-3 labeling of the equivalent confocal slice identified intracellular bacteria and host cell nuclei (merged image). Optical sections (0.5 μm thick) of cells transfected with siControl RNA revealed that exogenously added anti-CD63 antibody trafficked to and accumulated in TOPRO-3-positive chlamydial inclusions and resulted in reduced inclusion size (arrows). In cells transfected with siCD63 RNA and with the subsequent downregulation of CD63 expression (not shown), the exogenous anti-CD63 was excluded from the chlamydial inclusion (arrowheads) and accumulated in lysosomes (Lysotracker Red positive) with no alteration of inclusion development. The white line in the merged image indicates the position of the profile line used for the analysis of intensity distribution. Scale bar, 20 μm. (Right) Intensity distribution profiles confirmed that internalized anti-CD63 antibody (green line) displayed intensity levels above background at the site of the TOPRO-3-positive (blue line) chlamydial inclusion in siControl cells. In siCD63-infected cells, high intensity values for anti-CD63 (green line) localized with Lysotracker Red (red line) peripheral to the inclusion and host cell nuclei but displayed background intensity levels at the site of the chlamydial inclusion. The profile of the host cell nuclei indicates the background intensity levels of CD63 and Lysotracker Red.

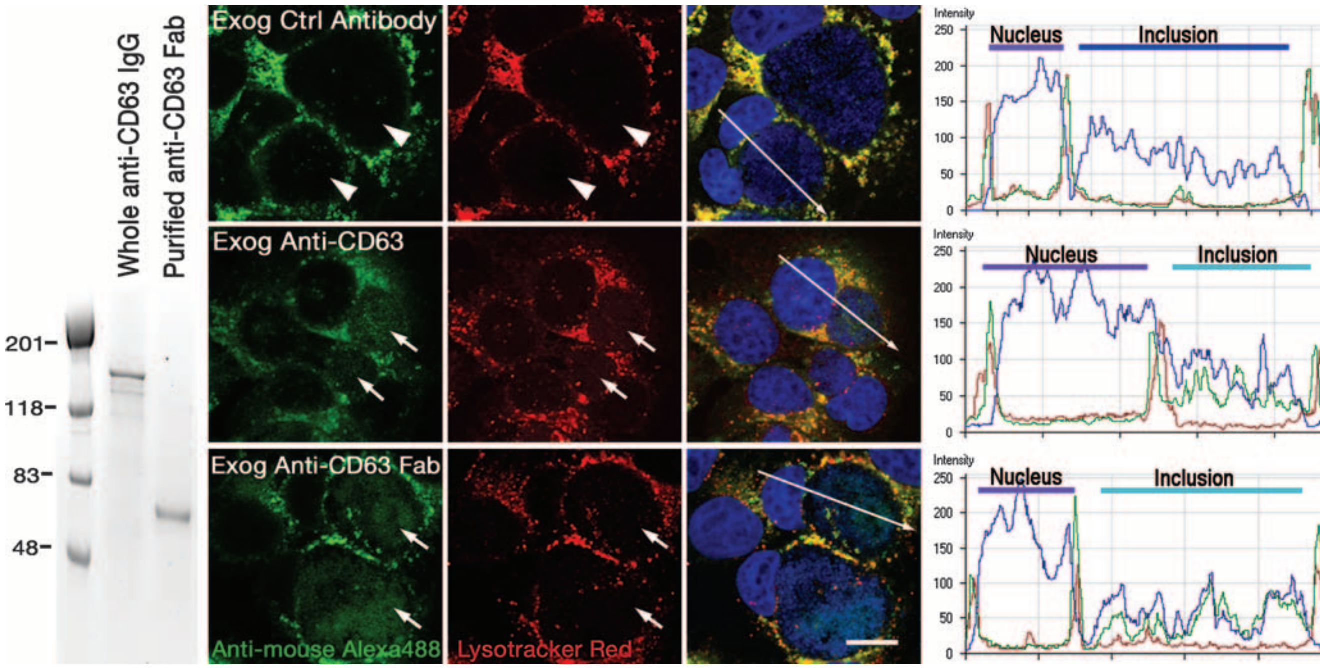

FIG. 7. Internalized exogenous (Exog) anti-CD63 Fab fragments localize to the chlamydial inclusion without the disruption of intracellular chlamydial development. (Left) A nonreducing SDS-PAGE gel of whole anti-CD63 Ig (150 kDa) and purified anti-CD63 Fab fragments (50 kDa). (Middle) HEp-2 cells infected with *C. trachomatis* E and cultured in the presence of the indicated exogenous antibody from 24 to 48 h postinfection. Infected cells were labeled with Lysotracker Red and then fixed and immunolabeled with fluorescein-conjugated anti-mouse IgG Fab fragment-specific antibody. The TOPRO-3 labeling of the equivalent confocal slice identified intracellular bacteria and host cell nuclei (merged image). Optical sections (0.8 μm thick) revealed that exogenously added control anti-LAMP-1 antibody was excluded from the chlamydial inclusion (arrowheads) and accumulated in lysosomes (Lysotracker Red positive). The exogenously added anti-CD63 antibody trafficked to perinuclear endocytic vesicles that generally did not colocalize with Lysotracker Red but accumulated in TOPRO-3-positive chlamydial inclusions (arrows) and resulted in reduced inclusion size. The exogenously added anti-CD63 Fab fragments trafficked to perinuclear endocytic vesicles (generally Lysotracker Red negative) and accumulated in TOPRO-3-positive chlamydial inclusions (arrows) with no alteration in inclusion size. The white line in the merged image indicates the position of the profile line used for the analysis of intensity distribution. Scale bar, 20 μm. (Right) Intensity distribution profiles of cells treated with control antibody showed high intensity values for anti-LAMP-1 (green line) localized with Lysotracker Red (red line) peripheral to the inclusion and host cell nuclei but displayed background intensity levels at the site of the chlamydial inclusion. In cells treated with anti-CD63 antibody or Fab fragments, intensity distribution profiles confirmed that internalized antibody (green line) displayed intensity levels above background at the site of the TOPRO-3-positive (blue line) chlamydial inclusion. The profile of the host cell nuclei indicates the background intensity levels of CD63 and Lysotracker Red. Ctrl, control.

anti-CD63 accumulated in perinuclear vesicular compartments and within the chlamydial inclusion (Fig. 6, upper). In addition, smaller inclusions were evident, confirming an effect of exogenous anti-CD63 antibody on inclusion development, as described previously (3). The analysis of cells transfected with siCD63, which were subsequently infected with *Chlamydia* and exposed to exogenously internalized anti-CD63, revealed variable inclusion sizes. Cells containing small inclusions with the incorporation of internalized antibody correlated with unaltered CD63 expression (data not shown) and expressed a phenotype identical to that of the siControl cells. In contrast, in siCD63-transfected cells, in which there was the subsequent downregulation of CD63 protein, exogenous anti-CD63 antibody did not localize to the chlamydial inclusion or alter intracellular chlamydial development (Fig. 6, lower). The distribution of anti-CD63 antibody was shown quantitatively by generating a profile of the intensity distribution along a line traversing the chlamydial inclusion (Fig. 6, right). As predicted, exogenously internalized anti-CD63 antibody failed to find an epitope in cells in which CD63 synthesis was blocked, resulting in endocytic trafficking to, and subsequent accumulation in, degradative lysosomes (Lysotracker Red positive).

To further analyze the discrepancy in outcome between these two approaches to neutralize CD63, the effects of exogenously internalized monovalent anti-CD63 Fab fragments were analyzed. Mouse anti-CD63 IgG1 antibody was fragmented using immobilized ficin protease, and subsequently Fab fragments were purified (Fig. 7, left). Exogenously internalized control antibody (anti-LAMP-1) trafficked to lysosomal compartments (Lysotracker Red positive) with no antibody localization to the chlamydial inclusion or alteration in chlamydial development (Fig. 7, top). Exogenously internalized whole divalent anti-CD63 antibody accumulated in perinuclear vesicular compartments and within the chlamydial inclusion, with a concurrent disruption in inclusion development (Fig. 7, center). An intermediate phenotype was observed when anti-CD63 Fab fragments were added to *Chlamydia*-infected cells. The monovalent Fab fragments accumulated in perinuclear vesicles and within the chlamydial inclusion; however, in contrast to whole divalent anti-CD63 antibody,

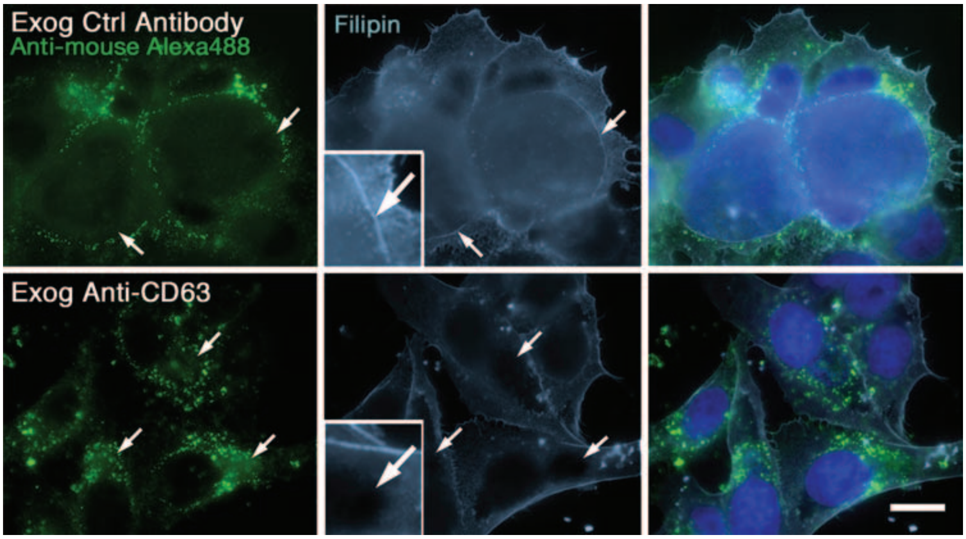

FIG. 8. Internalized exogenous (Exog) anti-CD63 antibody alters the distribution of cholesterol in *Chlamydia*-infected cells. HEp-2 cells infected with *C. trachomatis* serovar E and cultured in the presence of the indicated exogenous antibody from 24 to 48 h postinfection were fixed, labeled with anti-mouse Alexa Fluor 488 and filipin, and analyzed by fluorescence microscopy. TOPRO-3 labeling identified intracellular bacteria and host cell nuclei (merged image). (Upper) In cells cultured with exogenously added control anti-LAMP-1 antibody, filipin labeling showed the incorporation of cholesterol into *Chlamydia* and the inclusion membrane (arrows and insert). (Lower) Internalization of exogenous anti-CD63 antibody results in the disruption of chlamydial development with the lack of incorporation of cholesterol into the chlamydial inclusion (arrows and insert). Scale bar, 20 μm. Ctrl, control.

there was no evident alteration in inclusion development in confocal microscopy analyses. A quantitative comparison revealed a mean inclusion size of 538 μm^2 in the presence of Fab fragments and 312 μm^2 with exogenously added whole anti-CD63 antibody ($n = 50$). The distribution of anti-CD63 antibodies was shown quantitatively by generating a profile of the intensity distribution along a line traversing the chlamydial inclusion (Fig. 7, right). These studies indicate that both whole anti-CD63 antibody and monovalent Fab antibody fragments retain avidity for CD63 that is encountered within the endocytic pathway and traffic with this host protein. However, the disruption of inclusion development by undigested antibody suggests that the larger molecule, with its divalent structure and Fc portion, sterically hinders the functionality or transport of other components essential to MVB-to-inclusion delivery and subsequent inclusion biogenesis.

Internalized exogenous anti-CD63 antibody disrupts chlamydial growth and cholesterol acquisition. MVBs are pivotal in the mobilization of intracellular cholesterol, and the accumulation of anti-CD63 antibody within this compartment may indirectly interfere with cholesterol transport. To determine if an interruption in inclusion development by exogenous anti-CD63 antibody correlated with an interruption in cholesterol acquisition, inclusion development and filipin labeling were analyzed in cells cultured in the presence of the exogenous antibody. In cells cultured with control antibody (anti-LAMP-1), inclusions matured normally with cholesterol incorporation into the inclusion membrane (Fig. 8, upper). The internalized control anti-LAMP-1 antibody trafficked to lysosomal compartments with no antibody localization to the chlamydial inclusion according to fluorescence microscopy. In infected cells cultured in the presence of anti-CD63 antibody, as expected, the exogenous antibody localized to the sites of the *C. trachomatis* cells, and intracellular development was disrupted, as evidenced by the smaller inclusion size (Fig. 8, lower). However, under these conditions, the levels of cholesterol incorporation into *Chlamydia* and the inclusion membrane were not detectable by filipin labeling (Fig. 8, lower). The decrease in cholesterol incorporation in the presence of internalized anti-CD63 antibody paralleled the results observed with the MVB inhibitor U18666A (Fig. 3, lower). Both exogenous anti-CD63 antibodies and the MVB inhibitor blocked chlamydial development and altered the level of cholesterol incorporation into the inclusion. The filipin labeling of inclusions of equivalent size (i.e., for untreated cells and cells at 18 h postinfection) (Fig. 3, upper) indicated that cholesterol acquisition normally occurs early in development but is altered in the presence of exogenously added antibody or U18666A. These studies implicate cholesterol as a potential MVB-derived constituent that is important in intracellular chlamydial inclusion development.

DISCUSSION

The present study confirms the interaction between a CD63/LBPA-positive multivesicular compartment and intracellular chlamydiae with the direct delivery of resident host cell protein and lipid constituents to the lumen of the bacterial inclusion. The disruption of trafficking from these CD63-positive MVBs by a pharmacological inhibitor and exogenously internalized antibody subsequently reduced protein and cholesterol acquisition by the inclusion and delayed inclusion maturation with a marked reduction in infectious progeny. Neutralization with siRNAs and anti-CD63 Fab fragments revealed that CD63 itself was not required for the inclusion's novel interaction with lipid and cholesterol acquisition from these multivesicular host cell compartments. Collectively, these results indicate that

while cholesterol acquisition from MVBs is important for chlamydial growth, this process does not depend on CD63.

The tetraspanin protein CD63 is associated with both the internal vesicles and the limiting membrane of MVBs (8, 13) and previously was used as a surrogate marker for the analysis of the intersection of this compartment with the chlamydial inclusion (3). In parallel to this protein constituent, LBPA, a lipid highly enriched in internal vesicles of late endocytic multivesicular compartments (15), was analyzed in this study. LBPA-rich membranes have been proposed to play a role in the regulation of the transport of sphingolipids and cholesterol (14, 17), which are host-derived constituents acquired by the chlamydial inclusion (5, 6, 10, 24). Quantitative confocal studies revealed the colocalization of CD63 and LBPA in perinuclear compartments and accumulation at the site of the chlamydial inclusion (Fig. 1). Analysis at the ultrastructural level revealed CD63/LBPA-positive multivesicular organelles adjacent to the chlamydial inclusion. In addition, immunolabeling clearly showed CD63 and LBPA within the lumen of the inclusion at both 24 and 48 h postinfection. These constituents often were associated with interlumenal vesicles, implicating a direct fusion of MVBs with the chlamydial inclusion (Fig. 1).

Chlamydiae acquire host cell sphingomyelin and cholesterol from Golgi-derived vesicles destined for the plasma membrane (5, 6, 9, 10). The disruption of transport from the Golgi body does not completely disrupt chlamydial growth, indicating that this pathway of acquisition is not exclusive (6, 9). Previous studies defined an interaction between chlamydiae and MVBs that is essential for sphingolipid delivery to the maturing chlamydial inclusion (3). The present study analyzes MVBs as a source of cholesterol for the expanding inclusion. As described by Carabeo et al. (6), the distribution of cholesterol in infected cells can be visualized by using the fluorescent probe filipin. The labeling of infected cells with filipin results in the intense staining of the host cell plasma membrane and the inclusion membrane. The intracellular chlamydiae stain with a lower intensity that is difficult to document due to the photoinstability of the filipin probe. Here, filipin labeling revealed that the acquisition of cholesterol by the inclusion was disrupted when infected cells were cultured in the presence of the MVB inhibitor U18666A (Fig. 3). This pharmacological agent inhibits cholesterol transport from late endocytic compartments (19) and alters the trafficking of CD63 (11, 15, 16). In infected cells, U18666A treatment resulted in the dramatic accumulation of CD63 and cholesterol in enlarged perinuclear vesicles (Fig. 3), which correlated with the disrupted protein and cholesterol delivery to the chlamydial inclusion (Fig. 3) and a marked reduction of infectious progeny at 48 h postinfection (Fig. 2).

A functional role for CD63 in chlamydial inclusion biogenesis was suggested previously in studies that targeted the intracellular trafficking of this protein by using exogenously internalized anti-CD63-specific antibodies (3). Anti-CD63 antibodies accumulated in perinuclear compartments and subsequently trafficked to and incorporated in the chlamydial inclusion, demonstrating a direct interaction between CD63-positive MVBs and this bacterial compartment. In addition to this clear association, the exogenous antibody disrupted normal bacterial growth and inclusion maturation. To determine if the host cell protein CD63 was essential for the intersection of MVBs with the chlamydial inclusion, siRNA was used for the specific targeting and downregulation of CD63 within the infected host cell. Quantitative confocal studies and ultrastructural analysis revealed that the level of CD63 in MVBs and subsequent acquisition by the inclusion was dramatically reduced in siCD63-transfected cells (Fig. 4). Under these conditions, MVBs devoid of CD63 were clearly shown to intersect the chlamydial inclusion, with no alteration in host cell lipid or cholesterol acquisition by the inclusion and minimal effect on the growth of intracellular *Chlamydia* or the production of infectious progeny (Fig. 5). Despite its abundance in MVBs, siRNA studies confirmed that CD63 itself does not have a significant functional role in chlamydial inclusion biogenesis and likely serves as a passive marker in this novel pathway.

The discrepancy between results obtained using different methods of the neutralization of intracellular CD63 (siRNA and specific antibody) prompted the reevaluation of exogenous antibody uptake studies. As described in previous studies (3), the endocytic uptake of exogenous anti-CD63 antibody resulted in the accumulation of the antibody in the chlamydial inclusion coinciding with the disruption of inclusion development (Fig. 6). This observation is inconsistent with siRNA studies that clearly indicate that the neutralization of CD63 has no effect on inclusion maturation (Fig. 4). Therefore, the abundance of CD63 in MVBs, and the mass and divalence of the binding antibody, likely altered the transport or functionality of another MVB constituent imperative to nutrient delivery and inclusion biogenesis. This was confirmed by utilizing Fab fragments of the anti-CD63 antibody. These small, monovalent antigen-binding fragments efficiently penetrated the endocytic pathway and accumulated in late endocytic MVBs and the chlamydial inclusion (Fig. 7). However, unlike the intact Ig molecule, and in accordance with the siRNA studies, the Fab fragments had no effect on chlamydial inclusion development (Fig. 7). The tetraspanin protein CD63 likely traffics within contiguous membrane vesicles derived from MVBs, with divalent antibody binding to this protein and subsequently altering the functionality of adjacent components. The analysis of cholesterol distribution in infected cells treated with exogenous anti-CD63 antibody revealed a decrease in the accumulation of cholesterol at the inclusion membrane (Fig. 8). The internal membranes of MVBs are highly enriched with LBPA, a lipid thought to play a role in the regulation of the intracellular transport of cholesterol (13, 14), while the limiting membrane is enriched in MLN64, a cholesterol binding protein that mobilizes the transport of free cholesterol to acceptor membranes (1, 2, 12). CD63 is resident in both internal membranes and the limiting membrane of MVBs (8, 13). The abundance of CD63 and its proximity to MVB constituents essential to the mobilization of cholesterol may account for the effects of anti-CD63 antibody binding on chlamydial development. The potential role for LBPA and MLN64 in the interaction between CD63-positive MVBs and intracellular *Chlamydia* will be analyzed in ongoing studies.

Chlamydiae have a unique cycle of growth and replication that is completely contingent upon gaining a position in the intracellular environment of a eukaryotic host cell. The intricacies of the host cell's involvement in bacterial growth and inclusion biogenesis are not completely understood. De novo host cell protein synthesis is not required at any point during the developmental cycle; however, host cell-derived biosyn-

thetic precursors are imperative to the intracellular propagation and survival of chlamydiae. Obtaining these biosynthetic constituents from the host cell likely occurs by a multitude of acquisition mechanisms/strategies. One proposed source of essential constituents is via an interaction with MVBs, which are dynamic, heterogeneous, intermediate endocytic compartments that intersect the chlamydial inclusion serving as a source for sphingolipids and cholesterol. Deciphering the intricacies of the MVB and other pathways that allow for the bacterial acquisition of requisite host-derived constituents will have important implications on inclusion biogenesis and the therapeutic targeting of nutrient acquisition pathways that are crucial to the intracellular growth and subsistence of *Chlamydia*.

ACKNOWLEDGMENTS

Sincere thanks to Richard Morrison, Toshihide Kobayashi, and Jean Gruenberg for generously providing antibodies and L. David Sibley for comments on the manuscript.

This work was supported by an award from the American Heart Association.

REFERENCES

1. **Alpy, F., M. E. Stoeckel, A. Dierich, J. M. Escola, C. Wendling, M. P. Chenard, M. T. Vanier, J. Gruenberg, C. Tomasetto, and M. C. Rio.** 2001. The steroidogenic acute regulatory protein homolog MLN64, a late endosomal cholesterol-binding protein. J. Biol. Chem. **276:**4261–4269.
2. **Alpy, F., and C. Tomasetto.** 2006. MLN64 and MENTHO, two mediators of endosomal cholesterol transport. Biochem. Soc. Trans. **34:**343–345.
3. **Beatty, W. L.** 2006. Trafficking from CD63-positive late endocytic multivesicular bodies is essential for intracellular development of *Chlamydia trachomatis*. J. Cell Sci. **119:**350–359.
4. **Caldwell, H. D., J. Kromhout, and J. Schachter.** 1981. Purification and partial characterization of the major outer membrane protein of *Chlamydia trachomatis*. Infect. Immun. **31:**1161–1176.
5. **Carabeo, R. A., S. S. Grieshaber, E. Fischer, and T. Hackstadt.** 2002. *Chlamydia trachomatis* induces remodeling of the actin cytoskeleton during attachment and entry into HeLa cells. Infect. Immun. **70:**3793–3803.
6. **Carabeo, R. A., D. J. Mead, and T. Hackstadt.** 2003. Golgi-dependent transport of cholesterol to the *Chlamydia trachomatis* inclusion. Proc. Natl. Acad. Sci. USA **100:**6771–6776.
7. **Denzer, K., M. J. Kleijmeer, H. F. Heijnen, W. Stoorvogel, and H. J. Geuze.** 2000. Exosome: from internal vesicle of the multivesicular body to intercellular signaling device. J. Cell Sci. **113:**3365–3374.
8. **Escola, J. M., M. J. Kleijmeer, W. Stoorvogel, J. M. Griffith, O. Yoshie, and H. J. Geuze.** 1998. Selective enrichment of tetraspan proteins on the internal vesicles of multivesicular endosomes and on exosomes secreted by human B-lymphocytes. J. Biol. Chem. **273:**20121–20127.
9. **Hackstadt, T., D. D. Rockey, R. A. Heinzen, and M. A. Scidmore.** 1996. *Chlamydia trachomatis* interrupts an exocytic pathway to acquire endogenously synthesized sphingomyelin in transit from the Golgi apparatus to the plasma membrane. EMBO J. **15:**964–977.
10. **Hackstadt, T., M. A. Scidmore, and D. D. Rockey.** 1995. Lipid metabolism in *Chlamydia trachomatis*-infected cells: directed trafficking of Golgi-derived sphingolipids to the chlamydial inclusion. Proc. Natl. Acad. Sci. USA **92:**4877–4881.
11. **Higgins, M. E., J. P. Davies, F. W. Chen, and Y. A. Ioannou.** 2001. Niemann-Pick C1 is a late endosome-resident protein that transiently associates with lysosomes and the trans-Golgi network. Mol. Genet. Metabol. **68:**1–13.
12. **Kallen, C. B., J. T. Billheimer, S. A. Summers, S. E. Stayrook, M. Lewis, and J. F. Strauss III.** 1998. Steriodogenic acute regulatory protein (StAR) is a sterol transfer protein. J. Biol. Chem. **273:**26285–26288.
13. **Kobayashi, T., M. H. Beuchat, J. Chevallier, A. Makino, N. Mayran, J. M. Escola, C. Lebrand, P. Cosson, and J. Gruenberg.** 2002. Separation and characterization of late endosomal membrane domains. J. Biol. Chem. **277:**32157–32164.
14. **Kobayashi, T., M. H. Beuchat, M. Lindsay, S. Frias, R. D. Palmiter, H. Sakuraba, R. G. Parton, and J. Gruenberg.** 1999. Late endosomal membranes rich in lysobisphosphatidic acid regulate cholesterol transport. Nat. Cell Biol. **1:**113–118.
15. **Kobayashi, T., E. Stang, K. S. Fang, P. De Moerloose, R. G. Parton, and J. Gruenberg.** 1998. A lipid associated with the antiphospholipid syndrome regulates endosome structure and function. Nature **392:**193–197.
16. **Kobayashi, T., U. M. Vischer, C. Rosnoblet, C. Lebrand, M. Lindsay, R. G. Parton, E. K. Kruithof, and J. Gruenberg.** 2000. The tetraspanin CD63/lamp3 cycles between endocytic and secretory compartments in human endothelial cells. Mol. Biol. Cell **11:**1829–1843.
17. **Kolter, T., T. Doering, G. Wilkening, N. Werth, and K. Sandhoff.** 1999. Recent advances in the biochemistry of glycosphingolipid metabolism. Biochem. Soc. Trans. **27:**409–415.
18. **Kumar, Y., J. Cocchiaro, and R. H. Valdivia.** 2006. The obligate intracellular pathogen *Chlamydia trachomatis* targets host lipid droplets. Curr. Biol. **16:**1646–1651.
19. **Liscum, L., and J. R. Faust.** 1989. The intracellular transport of low density lipoprotein-derived cholesterol is inhibited in Chinese hamster ovary cells cultured with 3-beta-[2-(diethylamino)ethoxy]androst-5-en-17-one. J. Biol. Chem. **264:**11796–11806.
20. **Moorhead, A. R., K. A. Rzomp, and M. A. Scidmore.** 2007. The Rab6 effector Bicaudal D1 associates with *Chlamydia trachomatis* inclusions in a biovar-specific manner. Infect. Immun. **75:**781–791.
21. **Piper, R. C., and J. P. Luzio.** 2001. Late endosomes: sorting and partitioning in multivesicular bodies. Traffic **2:**612–621.
22. **Rzomp, K. A., L. D. Scholtes, B. J. Briggs, G. R. Whittaker, and M. A. Scidmore.** 2003. Rab GTPases are recruited to chlamydial inclusions in both a species-dependent and species-independent manner. Infect. Immun. **71:**5855–5870.
23. **Wolf, K., and T. Hackstadt.** 2001. Sphingomyelin trafficking in *Chlamydia pneumoniae*-infected cells. Cell. Microbiol. **3:**145–152.
24. **Wylie, J. L., G. M. Hatch, and G. Mcclarty.** 1997. Host cell phospholipids are trafficked to and then modified by *Chlamydia trachomatis*. J. Bacteriol. **179:**7233–7242.

Editor: R. P. Morrison